Articles

Controlling the Emission of Blue-Emitting Complexes by Encapsulation within Zeolite Cavities

Avelino Corma,* Urbano Díaz, Belén Ferrer, Vicente Fornés, María S. Galletero, and Hermenegildo García*

Instituto de Tecnología Química, UPV-CSIC, Universidad Politécnica de Valencia, Avda. de los Naranjos s/n, 46022 Valencia, Spain

Received August 18, 2003. Revised Manuscript Received January 26, 2004

Blue light-emitting boron 8-hydroxyquinolinate and 8-hydroxyquinaldinate complexes have been formed inside boron zeolites Beta, MCM-22, and ferrierite, and on layered ITQ-2 and ITQ-6 zeolites starting from the corresponding ligands and boron dislodged from framework positions. The luminescence properties, i.e., emission intensity, maximum wavelength, and lifetime of the ship-in-a-bottle quinolinate complexes are strongly modulated by the zeolite host. Besides the species responsible for the photoluminescence, other longer-lived transient species, presumably related to electron transport, are also photochemically generated and have been detected by laser flash photolysis.

Introduction

There has been an intense research effort aimed at the preparation of organic light-emitting diodes (OLEDs) exhibiting blue electroluminescence ($\lambda_{em} \approx 500$ nm) because of their potential application in full-color displays and screens.[1−6] The major advantage of OLEDs is their ease of processability and the possibility to obtain films rather than dots as in the current inorganic LEDs.[1,7] Besides organic polymers with *p*-phenylene and fluorene structure, metallic complexes are often used as LEDs.[8−10] Particularly important complexes are those derived from 8-hydroxyquinolinates (Q) as ligands and earth, rare earth, or transition metals.[11−24] The main advantage of these OLEDs is the ease of derivatization to modify and tune the photophysical properties to the target value by appropriate substitution on the ligand. For instance, in the case of 8-hydroxyquinolinate complexes it has been demonstrated that the emission wavelength varies depending on the metal radius, the coordination number, and the introduction of a methyl substituent at the 2-position of the Q ligand. As a general effect, it has been found that the weaker the metal−N bond in the complex, the bluer is the emission of the complex.

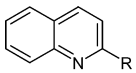

	R
Q	H
MQ	CH_3

It can be expected that the overall photostability, emission efficiency, and emission lifetime can be varied

* Primary authors. Address correspondence to A.C. Phone: 34 96 3877800. Fax: 34 96 3877809. E-mail: acorma@itq.upv.es.

(1) Heinrich, L. M. H.; Muller, J.; Hilleringmann, U.; Goser, K. F.; Holmes, A.; Hwang, D.; Stern, R. *Trans. Electron Devices* **1997**, *44*, 1249.
(2) Kido, J.; Okamoto, Y. *Chem. Rev.* **2002**, *102*, 2357−2368.
(3) Gaul, D. A.; Rees, W. S., Jr. *Adv. Mater.* **2000**, *12*, 935−946.
(4) Dirr, S.; Wiese, S.; Johannes, H. H.; Kowalsky, W. *Adv. Mater.* **1998**, *10*, 167−171.
(5) Sheats, J. R.; Antoniadis, H.; Hueschen, M.; Leonard, W.; Miller, J.; Moon, R.; Roitman, D.; Stocking, A. *Science* **1996**, *273*, 884−888.
(6) Strukelj, M.; Papadimitrakopoulos, F.; Miller, T. M.; Rothberg, L. J. *Science* **1995**, *267*, 1969−1972.
(7) Forrest, S. R. *Chem. Rev.* **1997**, *97*, 1793−1896.
(8) Thompson, M. E.; Lamansky, S.; Djurovich, P.; Murphy, D.; Abdel-Razzaq, F.; Forrest, S. R.; Baldo, M.; Burrows, P. E. *Polym. Mater. Sci. Eng.* **2000**, *83*, 202−203.
(9) Chen, C. H.; Shi, J. *Coord. Chem. Rev.* **1998**, *171*, 161−174.
(10) Hamada, Y. *IEEE Trans. Electron Devices* **1997**, *44*, 1208−1217.
(11) Hu, W.; Matsumura, M. *Appl. Phys. Lett.* **2002**, *81*, 806−807.
(12) Kwong, R. C.; Nugent, M. R.; Michalski, L.; Ngo, T.; Rajan, K.; Tung, Y.-J.; Weaver, M. S.; Zhou, T. X.; Hack, M.; Thompson, M. E.; Forrest, S. R.; Brown, J. J. *Appl. Phys. Lett.* **2002**, *81*, 162−164.
(13) Hu, W.; Manabe, K.; Furukawa, T.; Matsumura, M. *Appl. Phys. Lett.* **2002**, *80*, 2640−2641.
(14) Blochwitz, J.; Pfeiffer, M.; Hofmann, M.; Leo, K. *Synth. Met.* **2002**, *127*, 169−173.
(15) Jang, H.; Do, L. M.; Kim, Y.; Zyung, T.; Do, Y. *Synth. Met.* **2001**, *121*, 1667−1668.
(16) Yin, S.; Hua, Y.; Chen, X.; Yang, X.; Hou, Y.; Xu, X. *Synth. Met.* **2000**, *111−112*, 109−112.
(17) Chang, S.-C.; Liu, J.; Bharathan, J.; Yang, Y.; Onohara, J.; Kido, J. *Adv. Mater.* **1999**, *11*, 734−737.
(18) Bellmann, E.; Shaheen, S. E.; Thayumanavan, S.; Barlow, S.; Grubbs, R. H.; Marder, S. R.; Kippelen, B.; Peyghambarian, N. *Chem. Mater.* **1998**, *10*, 1668−1676.
(19) Hamada, Y. In *Organic Electroluminescent Materials and Devices*; Miyata, S., Nalwa, H. S., Eds.; Gordon and Breach: Amsterdam, the Netherlands, 1997; pp 311−334.
(20) Kido, J.; Hayase, H.; Hongawa, K.; Nagai, K.; Okuyama, K. *Appl. Phys. Lett.* **1994**, *65*, 2124−2126.
(21) Tao, X. T.; Suzuki, H.; Wada, T.; Sasabe, H.; Miyata, S. *Appl. Phys. Lett.* **1999**, *75*, 1655−1657.
(22) Tao, X. T.; Suzuki, H.; Wada, T.; Miyata, S.; Sasabe, H. *J. Am. Chem. Soc.* **1999**, *121*, 9447−9448.

10.1021/cm0347640 CCC: $27.50
Published on Web 03/04/2004

by incorporating the photolumophore complex in a host, because the intrinsic "molecular" photophysical properties of the emitter can be modified and controlled "supramolecularly" by its interaction with the host. In particular, competing radiationless deactivation decays arising from collision or conformational mobility are generally thwarted by immobilization on a rigid support leading as a general effect to an enhancement of the emission efficiency.[25,26]

Herein, we describe the ship-in-a-bottle synthesis of boron Q and MQ complexes encapsulated in a series of tridimensional (Beta, MCM-22, and Ferrierite) and novel bidimensional (ITQ-2 and ITQ-6) delaminated zeolitic materials and how their luminescence properties varied significantly from one zeolite to other. Our ship-in-a-bottle methodology is innovative because the boron is initially in zeolite framework positions and upon mild heating it becomes partially dislodged, and this coordination rearrangement permits the formation of new B−O bonds with Q or MQ complex located within the micropores.

Results and Discussion

For this work we have prepared a series of boron zeolites in which we have varied the zeolite structure and the boron content. A brief comment on the geometry of each of the zeolites employed in the present work is pertinent to understanding the ability of boron zeolites to form boron−quinolinate complexes. The internal pores of zeolite Beta are defined by oval cages of about 11 Å of longest axis defined by the intersection of two perpendicular 12-membered ring channels whose axes are somewhat shifted.[27] Zeolite MCM-22 structure also has oval cages (7.4 × 12 Å) that are accessible through 10-membered ring openings (∼5.3 Å).[28−31] Ferrierite (FER) contains two channel systems, one straight 10-ring channel (4.2 × 5.4 Å) intersected by a 8-membered ring channel.[27] Delaminated zeolites ITQ-2 and ITQ-6 are zeolitic materials that derive formally from delamination of laminar precursors of MCM-22 and FER, respectively.[32,33] The layers of ITQ-2 in particular contain open cups (5.4 × 6 Å) in which a guest can be accommodated. Figure 1 illustrates the structural relationship and pore structure of the zeolites used in the present work, and their main analytical and structural properties are summarized in Table 1.

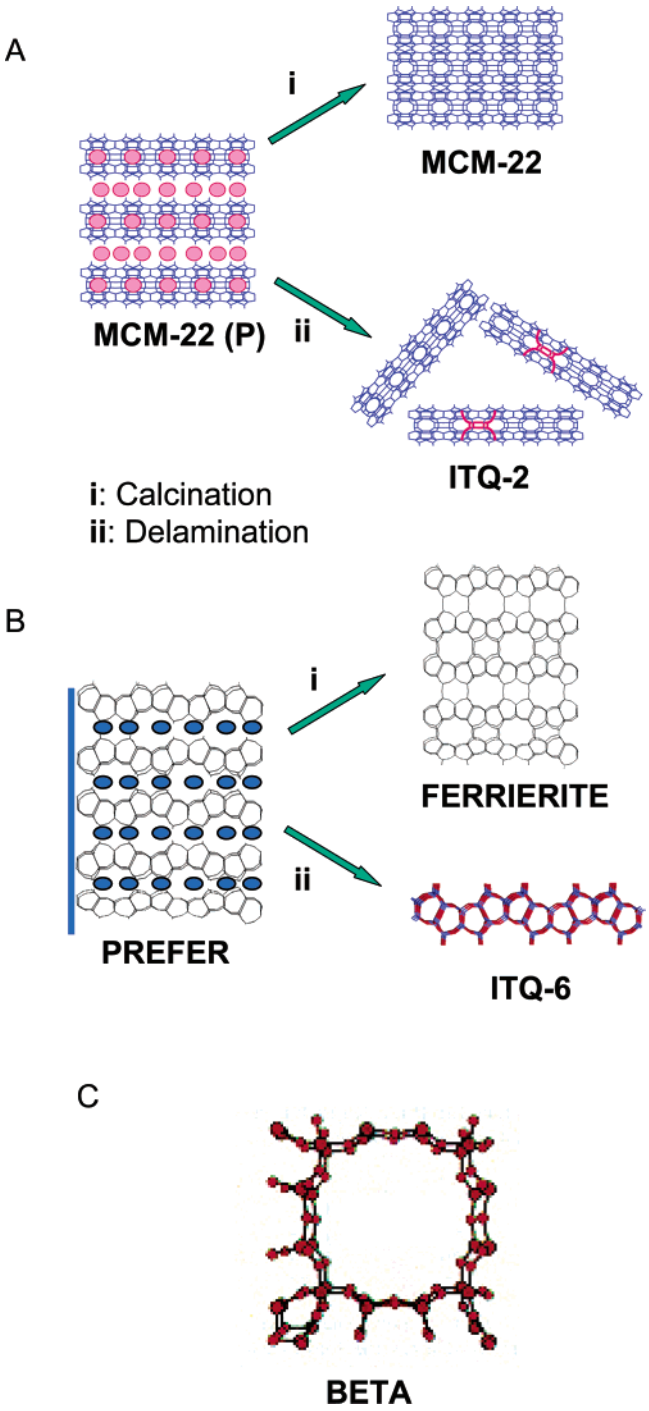

Figure 1. Structural relationship and pore structure of the zeolites used in this work. A: preparation procedure and structures of zeolites MCM-22 and ITQ-2; B: preparation procedure and structures of zeolites FER and ITQ-6; C: structure of zeolite Beta.

Herein, we demonstrate an innovative way to prepare encapsulated blue-emitting quinolinate complexes in which by starting from a crystalline, boron-containing zeolite, the corresponding ligand either Q or MQ is adsorbed, and then the system is submitted to mild heating at the required temperature to control the partial dislodging of B from framework positions. By doing this, it was intended that during the thermal reorganization of boron, formation of a boron−quinoli-

(23) A recent report has established that the structure of a previously reported blue electroluminescent borate complex, lithium tetra(2-methyl-8-hydroxyquinolato) boron, does not contain boron. Rather, it is the lithium salt of 2-methyl-8-hydroxyquinoline. For details see ref 24.

(24) Middleton, A. J.; Marshall, W. J.; Radu, N. S. *J. Am. Chem. Soc.* **2003**, *125*, 880−881.
(25) Scaiano, J. C.; García, H. *Acc. Chem. Res.* **1999**, *32*, 783−793.
(26) Garcia, H.; Roth, H. D. *Chem. Rev.* **2002**, *102*, 3947−4007.
(27) Meier, W. M.; Olson, D. H.; Baerlocher, C. *Zeolites* **1996**, *17*, 1−229.
(28) Nicolopoulos, S.; Gonzalez-Calbet, J. M.; Vallet-Regi, M.; Camblor, M. A.; Corell, C.; Corma, A.; Diaz-Cabanas, M. J. *J. Am. Chem. Soc.* **1997**, *119*, 11000−11005.
(29) Lawton, J. A.; Lawton, S. L.; Leonowicz, M. E.; Rubin, M. K. *Stud. Surf. Sci. Catal.* **1995**, *98*, 250−251.
(30) Nicolopoulos, S.; Gonzalez-Calbet, J. M.; Vallet-Regi, M.; Corma, A.; Corell, C.; Guil, J. M.; Perez-Pariente, J. *J. Am. Chem. Soc.* **1995**, *117*, 8947−8956.
(31) Unverricht, S.; Hunger, M.; Ernst, S.; Karge, H. G.; Weitkamp, J. *Stud. Surf. Sci. Catal.* **1994**, *84*, 37−44.
(32) Corma, A.; Fornés, V.; Pergher, S. B.; Maesen, T. L. M.; Buglass, J. G. *Nature* **1998**, *396*, 353−356.
(33) Corma, A.; Diaz, U.; Domine, M. E.; Fornes, V. *Angew. Chem., Int. Ed.* **2000**, *39*, 1499−1501.

Table 1. Analytical and Structural Properties of the Zeolites Used in This Work

	BET (m^2/g)	micropore volume (cm^3/g)	Si/B
(B)MCM-22	400	0.16	12
(B)ITQ-2	700	0.09	12
(B)Beta	460	0.19	50
(B)FER	279	0.10	25
(B)ITQ-6	595	0.03	12

Scheme 1

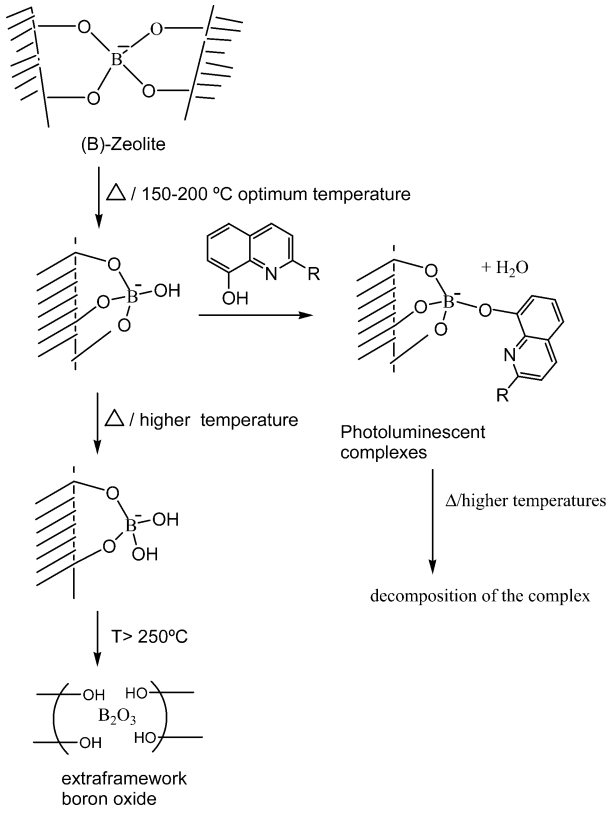

nate complex would occur as indicated in Scheme 1. If the heating temperature were increased more than the required optimum, then undesirable massive deboronation with formation of nonemissive boron oxide clusters as well as thermal decomposition of the boron−quinolinate complex would occur.

According to the equation shown in Scheme 1, it should be possible to control the properties of the complex, including the photoluminescence properties, in at least three ways besides the obvious one of changing the ligand: (i) by varying the zeolite structure and the space available for the formation of the boron−quinolinate complex (either 1:1 or 1:2 stoichiometry); (ii) by controlling the extraframework migration of the boron (temperature of the migration), and (iii) by varying the boron content of the zeolite. As we will show below, our expectations were indeed realized. What is important to note is that an effective control of the "intrinsic" photoluminescence of the boron−quinolinate complex is achieved by embedding it inside zeolite hosts of different structure.

The procedure followed for the ship-in-a-bottle synthesis of the boron−quinolinate complexes was the same in all cases and consists of heating (typically at 200 °C) a mechanical mixture of a given amount of Q or MQ (typically 5 wt %) and the boron-containing zeolite for a period of 4 h. We observed that higher calcination temperatures do not increase further the photoluminescence of the solid as indicated in Scheme 1. After the thermal treatment, the solid sample was submitted to exhaustive solid−liquid extraction to remove uncomplexed Q or MQ ligand. In no case was any product observed in the extract other than unreacted ligand. For the ligand/zeolite ratios studied, no ligand was recovered for (B)Beta and (B)MCM-22, suggesting that the adsorption has been successful and that the boron complex has been formed. The large size of the resulting BQ complex and/or its covalent binding to the zeolite framework should impede the complex from diffusing outside the zeolite, and, therefore, BQ would remain unextractable inside the zeolite voids or on the zeolite cups.

Table 2. Combustion Analysis and Absorption Maximum (λ_{LMCT}) of the Quinolinate Samples Prepared

	% N	% C	λ_{LMCT}
BQ@Beta	0.51	4.30	364
BMQ@Beta	0.40	3.35	365
BQ@MCM-22	0.46	3.86	362
BMQ@MCM-22	0.10	0.81	357
BQ@ITQ-2	0.26	2.01	358
BMQ@ITQ-2	0.23	1.83	360
BQ@FER	0.07	0.43	[a]
BQ@ITQ-6	0.20	1.70	364

[a] Not observed.

This interpretation agrees with the subsequent characterization of the solids (see below). In contrast, in the case of medium-pore- size (B)FER most of the ligand could not enter the pores, instead remaining on the external surface without reacting with framework B, and it was recovered after the thermal treatment by the solid extraction.

In the case of the layered (B)ITQ-2 and (B)ITQ-6 a percentage of the Q or MQ ligands is recovered in the extraction, but a significant amount of the ligands still remains adsorbed after the extraction. Blank controls in which an analogous mechanical mixture of the ligands and (B)ITQ-2 or (B)ITQ-6 (not heated) was thoroughly extracted indicates that over 90% of the ligands are recoverable by our extraction protocol. Thus, we suggest that for (B)ITQ-2 or (B)ITQ-6, the fraction of unextractable Q and MQ should correspond to that actually forming boron complexes, and that the covalent bonding of the boron atoms to the framework is responsible for the failure of the complete recovery of the ligand in agreement with Scheme 1. Interestingly, (B)ITQ-2 that has a structured surface formed by cups of $\sim 7 \times 8$ $Å^2$ retains significantly larger amounts of ligands than the analogous delaminated material (B)ITQ-6 that does not present such "cups" at the surface. Comparison of the loadings achieved for (B)ITQ-2 and (B)ITQ-6 suggests that Q and MQ are not retained because of adsorption on the large external surface of the delaminated zeolites, but it really takes place in the external cup-type cavities of the (B)ITQ-2. The final Q or MQ loading of the complexes was determined by combustion C and N analysis and some of the data are collected in Table 2 to give an idea of the typical loading obtained for each boron-containing zeolite under the standard preparation procedure.

Firm evidence that the presumed boron−quinolinate complex has been formed during the ship-in-a-bottle

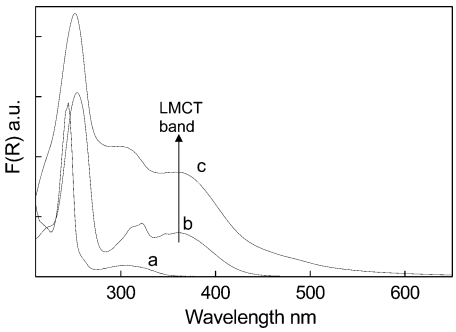

Figure 2. Optical (transmission, curve a) spectrum of Q in CH_2Cl_2 solution and diffuse reflectance UV−Vis spectra (plotted as the Kubelka−Munk function of the reflectance) of the samples BMQ@ITQ-2 (b) and BQ@Beta (c). The plot shows the characteristic ligand-to-metal charge transfer (LMCT) band specific of the boron−quinolinate complexes.

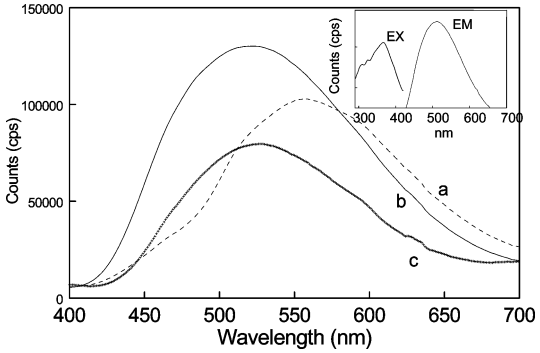

Figure 3. Emission spectra (λ_{ex} = 360 nm) of the samples BQ@MCM-22 (a), BQ@ITQ-2 (b), and BMQ@ITQ-2 (c) recorded under the same conditions. The inset shows the emission (EM λ_{ex} = 360 nm) and the excitation (EX λ_{em} = 510 nm) spectra of the sample BMQ@MCM-22.

synthesis and remains encapsulated after the extraction can be obtained by diffuse reflectance UV−Vis (DRUV) spectroscopy. Figure 2 shows the DRUV of two representative samples prepared in the present work. For the sake of comparison the transmission UV/Vis spectrum of Q has also been included. As can be seen in this Figure 2 after addition of Q and mild heating, the boron zeolite samples exhibit a ligand-to-metal charge transfer (LMCT) absorption band at about 360 nm, absent in the starting zeolites or ligands, and that is characteristic of the metal−quinolinate complexes as reported in the literature.[22] Table 2 also lists the actual λ_{LMCT} for this band.

In agreement with the DRUV spectra of the BQ@ zeolite or BMQ@zeolite samples, all the solids exhibit intense emission upon excitation at the corresponding λ_{LMCT} (∼360 nm). Figure 3 shows four selected emission spectra of boron−quinolinate complexes encapsulated in zeolites recorded under identical conditions. In each case, the excitation spectrum obtained monitoring at the emission maximum coincides with the LMCT band of the boron−quinolinate complex in the absorption spectrum (inset of Figure 3), thus confirming these boron complexes as the actual emitting species. Blank controls demonstrate that this intense emission is totally absent when the same preparation procedure is followed using zeolites lacking boron in their structure.

Two important features arise from the emission measurements. First, the emission intensity recorded under identical experimental conditions depends not

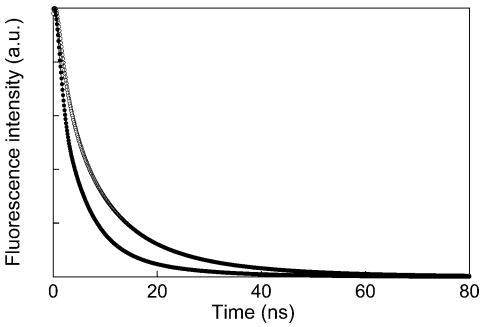

Figure 4. Emission decays monitored at the corresponding λ_{em} of the N_2-purged samples BMQ@MCM-22 (○) and BQ@MCM-22 (●).

only on the ligand loading (Table 2), but on the pore dimensions and geometry of the zeolite. The spatial constraint certainly will have an effect on the structure of boron−quinolinate complexes (bond distances and angles) and/or on the level of confinement and consequently on the emission quantum yields.[25,34] As mentioned earlier, variations on the structure and bonding of the boron−quinolate complexes are manifested in the emission properties of these complexes.

The second emission feature observed was that the maximum emission intensity wavelength (λ_{em}) also varies significantly in a range of 50 nm from one zeolite to another. The λ_{em} value is an important parameter because the luminescence color is related to this value. Herein, Figure 3 demonstrates that by simply varying the zeolite host, a certain degree of control in λ_{em} can be achieved. Target values for λ_{em} are about ∼500 nm. There are two reasons that can explain the variations in the λ_{em} by varying the zeolite host. The first is the zeolite confinement effect consisting in the perturbation of HOMO−LUMO band gaps by incorporation of a guest in a restricted space.[35] This confinement effect has been demonstrated to be responsible for variations of the λ_{em} of naphthtalene,[36] anthracene,[37] and diazabicycloheptene[38] within zeolites of different spaces. The second possible reason is variation in the structure and stoichiometry of the actual boron−quinolinate emitters.

A general methodology to learn about the distribution of photolumophores among different populations is to study the temporal profile of the emission. Figure 4 shows two selected emission decays monitored at the corresponding λ_{em} of the sample. Emission decays were fitted to three superimposed first-order kinetics. The calculated τ values and corresponding populations are collected in Table 3 and they also reflect once again the influence of zeolite host on the kinetics decay. Figure 4 also shows the theoretical fittings from which the lifetimes and population distribution have been obtained. Comparison of the experimental decays and theoretical fitting gives a visual indication of the quality kinetic analysis.

(34) Garcia, H.; Roth, H. D. *Chem. Rev.* **2002**, *102*, 3547.
(35) Corma, A.; Zicovich-Wilson, C.; Viruela, P. *J. Phys. Chem.* **1994**, *98*, 10863−10870.
(36) Márquez, F.; García, H.; Palomares, E. J.; Fernández, L.; Corma, A. *J. Am. Chem. Soc.* **2000**, *122*, 6520−6521.
(37) Márquez, F.; Zicovich-Wilson, C. M.; Corma, A.; Palomares, E. J.; Garcia, H. *J. Phys. Chem. B* **2001**, *105*, 9973−9979.
(38) Márquez, F.; Marti, V.; Palomares, E. J.; Garcia, H.; Adam, W. *J. Am. Chem. Soc.* **2002**, *124*, 7264−7265.

Table 3. Photoluminescence Data of the Encapsulated Boron Complexes (Numbers in Brackets Correspond to the Relative Percentage of the Lifetime Contributing to the Overall Signal Decay)

	λ_{em} (nm)	τ_1 (ns)	τ_2 (ns)	τ_3 (ns)
BQ@MCM-22	557	7.33 (44.63%)	1.65 (11.80%)	18.90 (43.58%)
BMQ@MCM-22	507	0.34 (23.61%)	4.45 (46.65%)	14.23 (39.74%)
BQ@ITQ-2	524	1.08 (16.16%)	5.49 (58.1%)	13.91 (25.75%)
BMQ@ITQ-2	518	1.46 (13.49%)	6.61 (52.55%)	16.89 (33.96%)
BMQ@Beta	550	13.54 (30.57%)	5.31 (44.11%)	1.40 (25.32%)

From the above emission data it can be concluded that (B)MCM-22 and (B)ITQ-2 are the most suitable host materials for boron−quinolinate complexes in terms of shorter wavelength emission and higher intensity. The two solids are morphologically related (Figure 1) and they contain one open half cavity at the external surface (ITQ-2 and MCM-22) plus a complete closed cavity with 10-membered ring openings with the same internal diameter for MCM-22. Assuming that the complex is located inside these cavities, geometry optimization at the semiempirical AM1 level and molecular modeling using molecular mechanics of the zeolite cluster and the complex indicate that the boron complex can only have a 1-to-1 boron/quinolinate ligand stoichiometry. Figure 5 shows a visualization of BQ complex located on (B)ITQ-2 cups. As far as we know, this 1-to-1 stoichiometry for the BQ or BMQ complexes has never been reported in solution and can only be accomplished because of the restricted space available in the interior of the zeolite pores. Precedents in which the stoichiometry of the europium complexes change depending on the zeolite cavity size can be found in the literature.[39,40] Concerning the influence of the complex stoichiometry on the emission properties, it should be reminded that the LMCT electronic transition from which the emission arises is a property that, in principle, requires only a single boron−quinolinate moiety.

Concerning the influence of the nature of the quinolinate ligand on the emission of the encapsulated complexes, this is only marginal in the case of (B)MCM-22 and (B)ITQ-2, whereas it plays a notable effect in the case of the large pore size (B)Beta zeolite. In solution, the change from Q to MQ produces a significant shift in λ_{em} toward the desired blue as a consequence of the weakening of the undesirable boron−nitrogen bond. The fact that there is a notable shift between Q and MQ for (B)Beta can be rationalized considering that in this large pore zeolite, due to the larger dimensions of the internal void spaces, Q can interact with boron atoms such as in solution through the O and N atoms, whereas due to the steric constraints in (B)MCM-22 and (B)ITQ-2 only the O atom interacts. The absence of λ_{em} shift for BQ and BMQ recorded for (B)MCM-22 and (B)ITQ-2 relative to (B)-Beta could reflect that there is no occurrence of boron−nitrogen interactions in MCM-22 or ITQ-2 zeolites. Then, the change in the ligand from Q to MQ should not produce any effect in (B)MCM-22 or (B)ITQ-2, but it could be reflected in the emission of (B)Beta. Another difference between the ligands related to a more impeded diffusion of MQ relative to Q inside the pores is a decrease in the loading for MQ that is accompanied by a significant decrease in the emission intensity.

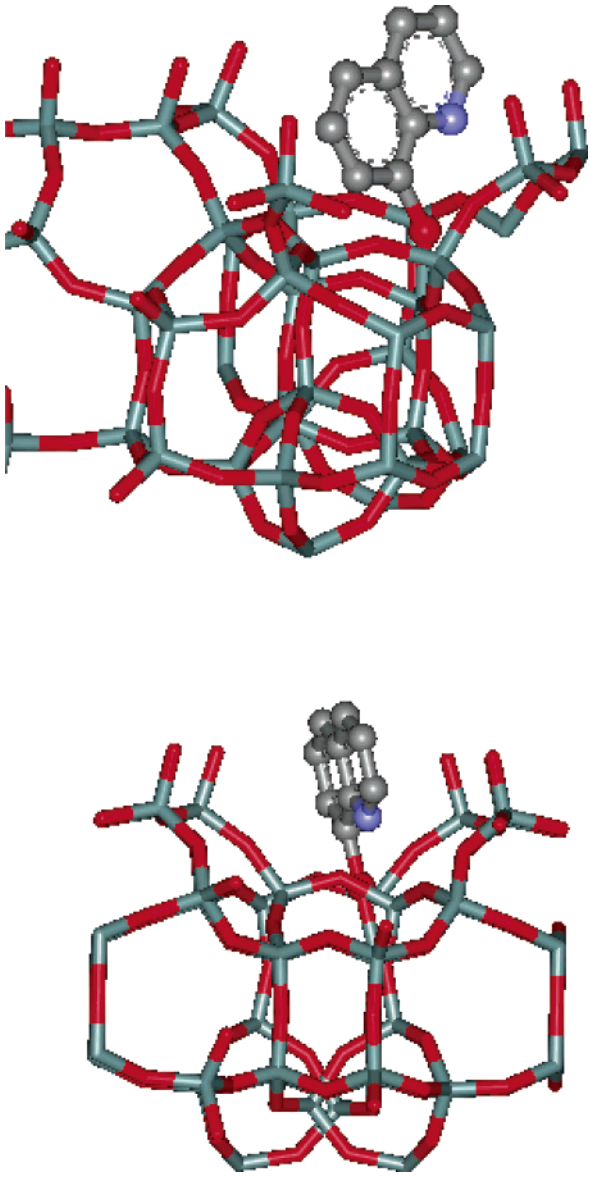

Figure 5. Two views of molecular modeling of the ligand Q covalently bonded to framework boron inside the ITQ-2 cups.

Our photochemical study of the BQ and BMQ complexes adsorbed on zeolites was completed by performing laser flash photolysis of the BQ@ITQ-2 and BMQ@ITQ-2 as two selected samples. It has been reported that in OLEDs,[41] quinolinate complexes act as the light-emitting layer and also as the electron transport layer. The electron transport ability of an organic compound or a metallic complex is frequently related to the occurrence of thermal or photoinduced electron-transfer processes with the intermediacy of the corresponding

(39) Alvaro, M.; Fornés, V.; García, S.; García, H.; Scaiano, J. C. *J. Phys. Chem. B* **1998**, *102*, 8744−8750.

(40) Hashimoto, S.; Kirikae, S.; Tobita, S. *Phys. Chem. Chem. Phys.* **2002**, *4*, 5856−5862.

(41) Heinrich, L. M. H.; Muller, J.; Hilleringmann, U.; Goser, K. F.; Holmes, A.; Hwang, D.; Stern, R. *Trans. Electron Devices* **1997**, *44*, 1249−1252.

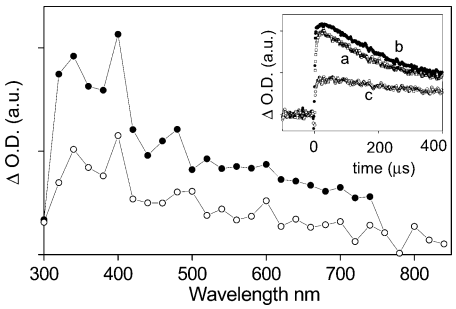

Figure 6. Transient diffuse reflectance UV−Vis spectra of the sample BQ@ITQ-2 recorded 30 (●) and 300 (○) μs after 355 nm laser excitation under N_2 atmosphere. The inset shows the decays monitored at 340 (a), 400 (b), and 500 (c) nm.

Scheme 2

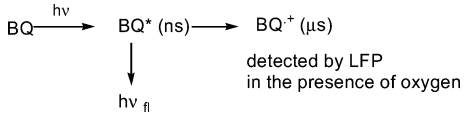

radical ions. Thus, we submitted the encapsulated boron−quinolinate complexes to nanosecond laser flash photolysis that is a fast technique with submillisecond time resolution allowing detection of short-lived reaction intermediates.[42,43] In fact, upon 355-nm laser excitation, the generation of transient species decaying in hundreds of microseconds was detected (Figure 6). It is interesting to note that the species responsible for the spectra of Figure 6 have to be different from the excited-state responsible for the emission, since the lifetime and temporal profiles of the emitting excited states are in the nanosecond time scale. Thus, light absorption causes at least two different phenomena. In a percentage of cases, some photons absorbed by the boron-complex are re-emitted as photoluminescence, but in some other cases, light absorption originates different species as indicated in Scheme 2.

Careful inspection of the signal decay recorded at different wavelengths upon laser excitation shows that the profile varies depending on the wavelength, indicating that there is more than a single intermediate. It is worth noting at this point that typical organic radical cations are not quenched by oxygen. Therefore, the signal recorded in the presence of oxygen can be due to radical cations. Moreover, oxygen quenches the signal differently depending on each wavelength. Figure 7 shows some selected decays to illustrate the previous point. Although an exhaustive study is still necessary to fully understand the transient spectra recorded by laser flash photolysis, all the available data support that besides the emitting excited state, light absorption produces longer lived species that can be responsible for the electron transport ability of the quinolinate complexes (particularly those not quenched by oxygen). We propose that one of the transients observed could be the species generated by electron photoejection from the complex as indicated in Scheme 3. The electron would be captured by framework electron acceptor sites

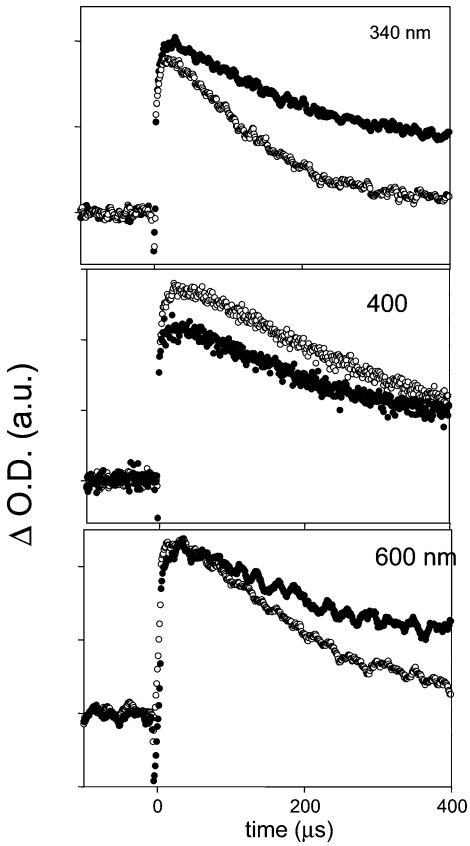

Figure 7. Decays monitored at different wavelengths (340, 400, and 500 nm) recorded under N_2 (●) and O_2 (○) atmosphere after 355 nm excitation of the sample BQ@ITQ-2.

Scheme 3

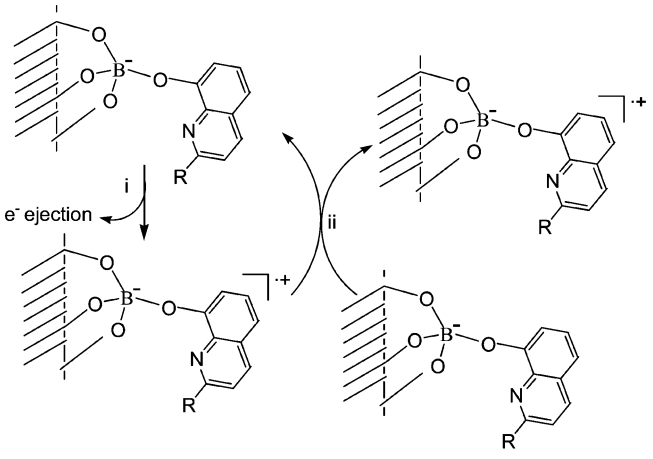

or by charge compensating cations, a phenomenon that has been previously observed to occur in zeolites.[26] Then, the electron transport would take place through electron hoping from a photogenerated radical cation to a neighbor boron complex (Scheme 3). The above results indicated that the zeolite entrapped quinolinate complexes also exhibit the dual behavior observed for the nonencapsulated complexes.

With the above data at hand, a preliminary test of BMQ@ITQ-2 as electroluminescent active layer was carried out by preparing a film of this solid by dipcoating it onto an ITO electrode, using Al as back electrode.

(42) Wilkinson, F.; Kelly, G. In *Handbook of Organic Photochemistry*; Scaiano, J. C., Ed.; CRC Press: Boca Raton, FL, 1989; Vol. 1, p 293.

(43) Bohne, C.; Redmond, R. W.; Scaiano, J. C. In *Photochemistry in Organized and Constrained Media*; Ramamurthy, V., Ed.; VCH: New York, 1991; pp Chapter 3, pp 79−132.

Working at high voltages (12 V), a electroluminescence emission (λ max 500 nm) was recorded, thus, demonstrating the potential of zeolite encapsulated in LEDs.

In summary, we have demonstrated that blue-emitting boron quinolinate complexes can be prepared by ship-in-a-bottle synthesis inside zeolites or on the open cavities or pores at the surface of layered zeolites through a strategy based on the thermally promoted deboronation of framework boron zeolites. We have shown that emitting properties, such as emission intensity, maximum wavelength, and emission lifetimes, are strongly modulated by the zeolite host. Among the series studied, zeolites MCM-22 and ITQ-2 are the most promising hosts for this purpose. Besides photoluminescence, other longer-lived transient species presumably related to electron transport are also photochemically generated. Electroluminescence has been observed for the BMQ@ITQ-2 films deposited on ITO electrode.

Experimental Section

The boron-containing beta, pre-MCM-22, and pre-ferrierite zeolites used in this work have been prepared in our laboratory following the hydrothermal crystallization procedure previously reported in the literature for the synthesis of each material,[32,44,45] with the only difference of the presence of $B(OH)_3$ as boron source in the mother gel. Upon calcinations under air at 650 °C, pre-MCM-22 and pre-ferrierite render the corresponding (B)MCM-22 and (B)ferrierite used in this work (Table 1). Alternatively, the layered pre-MCM-22 and pre-ferrierite were ion-exchanged with cetyltrimethylammonium and the swolled materials submitted to ultrasonic irradiation as described[32,33] to obtain the delaminated (B)ITQ-2 and (B)-ITQ-6, respectively. The Si/B ratio of the crystallization gel was varied in the range 50 to 10.

Characterization Techniques. Chemical analyses (C, N, H) were carried out by combustion using a Perkin-Elmer analyzer. Diffuse reflectance UV−Vis spectra of pressed powders were recorded on a Cary 5G spectrophotometer using a praying mantis accessory and $BaSO_4$ as standard. Fluorescence spectra and emission lifetimes were recorded on an Edinburgh Analytical Instruments FL900 spectrophotometer. Laser flash photolysis experiments were carried out using the third (355 nm, $\leq$ 20 mJ$\times$pulse^{-1}) harmonic of a Surelite Nd:YAG laser for excitation (pulse $\leq$ 10 ns). The signal from the monochromator/photomultiplier detection system was captured by a Tektronix 2440 digitizer and transferred to a computer that controlled the experiment and provided suitable processing and data storage capabilities.

Acknowledgment. Financial support by the Spanish DGES (Project MAT2003-1226) and Generalidad Valenciana (grupos03-020) is gratefully acknowledged. B.F. also thanks the Spanish Ministry of Education for a postgraduate scholarship.

CM0347640

(44) Camblor, M. A.; Mifsud, A.; Pérez-Pariente, J. *Zeolites* **1991**, *11*, 792−797.

(45) Corma, A.; Díaz, U.; Domine, M. E.; Fornés, V. *J. Am. Chem. Soc.* **2000**, *122*, 2804−2809.